Mechanics of Structures and Machines

An International Journal

MECH. STRUCT. & MACH., 29(2), 199–221 (2001)

TOPOLOGY OPTIMIZATION OF COMPLIANT MECHANISMS WITH STRENGTH CONSIDERATIONS*

A. Saxena and G. K. Ananthasuresh†

Department of Mechanical Engineering and
Applied Mechanics, University of Pennsylvania,
Philadelphia, Pennsylvania 19104-6315

ABSTRACT

Multicriteria formulations that have been reported previously in topology design of compliant mechanisms address flexibility and stiffness issues simultaneously and aim to attain an optimal balance between these two conflicting attributes. Such techniques are successful in indirectly controlling the local stress levels by constraining the input displacement. Individual control on the conflicting objectives is often difficult to achieve with these flexibility-stiffness formulations. Resultant topologies may sometimes be overly stiff, and there is no guarantee against failure. Local stresses may exceed the permissible yield strength of the constituting material in such designs. In this article, local failure conditions relating to stress constraints are incorporated in topology optimization algorithms to obtain compliant and strong designs. Quality functions are employed to impose stress con-

*Communicated by S. Azarm.
†Corresponding author. Fax: (215) 573-6334; E-mail: gksuresh@seas.upenn.edu

straints on retained material, ignoring nonexisting regions in the design domain. Stress constraints are further relaxed to regularize the design space to help the mathematical programming algorithms based on the Karush-Kuhn-Tucker conditions yield improved solutions. Examples are solved to corroborate the solutions for failure-free compliant topologies that are much improved in comparison to those obtained using flexibility-stiffness multicriteria objectives.

I. INTRODUCTION

Numerous advantages associated with compliant mechanisms [1,2] recently have motivated researchers toward their design. An approach to designing monolithic compliant mechanisms is their topology synthesis [3–6], which seeks an optimal material distribution over a specified design region, called the *design domain*, for prescribed functional performance, that is, their ability to transmit motion and/or forces solely using the elastic deformation of the constituting members. Topology design of compliant mechanisms has been accomplished in the past by using flexibility-stiffness multicriteria formulations. These formulations intend an optimal balance between the flexibility and stiffness in the resulting continua to obtain the force/motion transmission capabilities.

Ananthasuresh [3] quantified the flexibility of a compliant continuum as the output displacement and used strain energy as a metric for its stiffness. The larger the output displacement, the more flexible is the optimal continuum; similarly, the smaller the strain energy, the stiffer it is.

To facilitate the use of Euler-Lagrange principles of variational calculus, Ananthasuresh [3] employed the virtual work method to compute the output displacement as the mutual strain energy [7]. For optimal simultaneous flexibility and stiffness of a compliant continuum, he proposed a multicriteria scheme to optimize a weighted linear combination of the two objectives.

An improved objective of maximizing the ratio of the output displacement and strain energy was proposed by Frecker et al. [4]. Frecker et al. [8] further suggested a two-stage procedure for optimal topology design in which, in the first stage, an optimal topology was obtained using the ratio formulation and was improved subsequently using the optimality criteria method in which the strain energy density was made uniform throughout the continuum.

Saxena and Ananthasuresh [9] addressed the flexibility, stiffness, and mechanical advantage aspects of a compliant continuum simultaneously by proposing an energy formulation. Here, the flexibility of the continuum was modeled as the energy stored in the spring that models the output forces or, equivalently, the square of the output deformation.

Saxena and Ananthasuresh [6] generalized the measures for both the flexibility and stiffness of a continuum as monotonic functions of the output displacement and strain energy, respectively, and derived a structural property for optimal compliant topologies with the linear combination and ratio multicriteria formulations. The property states that for a compliant topology to be optimally flexible and stiff, the ratio of the mutual strain energy and strain energy densities is uniform throughout the continuum but for portions that are otherwise bounded by upper and lower bounds on the design variables. This property was used in the optimality criteria setting to resize the design variables. It was also noted that the flexibility-stiffness multicriteria formulations are often nonconvex, and therefore a robust one-variable search was incorporated to make the algorithm reliable and robust.

Another optimality criteria method to design flexible-stiff compliant topologies was by Canfield and Frecker [10], who employed a resource constraint in the optimization statement. A formulation similar to the flexibility-stiffness scheme was proposed by Sigmund [5], who employed a constraint on the input displacement while maximizing the output deformation.

A. Compliant and Strong

The *strength* of a part is its ability to prevent failure when subjected to external loads. Both the geometry and material properties determine the strength of a part. Numerous theories predicting failure for ductile and brittle materials are well established in engineering design practice, a few being the Rankine, Tresca, and von Mises distortion energy theories [11]. Rankine theory, applicable mostly to brittle materials, states that failure occurs when the maximum principal stress in a continuum exceeds the yield stress of the material; for ductile materials, Tresca theory predicts failure when the maximum shear stress exceeds the yield limit. The most commonly used theory is the distortion energy theory, which postulates that failure occurs when the von Mises stress exceeds the yield strength of the material.

From the design perspective, given the magnitudes of the external loads applied, the part geometry and the material properties should be appropriately chosen to restrict the local stress levels within the yield stress. Such designs can be determined using indirect approaches, for instance, by maximizing the stiffness (or equivalently minimizing the strain energy) or by employing direct methods, that is, by incorporating stress constraints in the optimization statement. Minimization of strain energy is sought mainly when the primary intent is to design structures for minimal deformation, for instance, overpasses, skyscrapers, and dams. The outcome of the strain energy minimization is the restrained overall displacement field that indirectly restrains stresses, but not necessarily to

plished by either increasing the cross-sectional area bt, which makes the beam stiffer, or by decreasing the elastic modulus E, consequently making it compliant. Making the area of cross section of the beam variable along the length leads to more possibilities of creating compliant and strong designs.

Maximizing stiffness in the flexibility-stiffness multicriteria formulations when designing compliant mechanisms is not appropriate for two reasons. First, strain energy minimization interferes directly with the primary design intent of maximizing the flexibility of a compliant continuum as it leads to a more restricted overall deformation field. Consequently, the optimal compliant continuum may be overly stiff. Second, minimizing the strain energy alone fails to account for the local failure, which is essential in dealing with elastic members undergoing large deformation. A more direct approach of achieving flexibility while simultaneously addressing local failure issues is by maximizing the output deformation while restricting the local stresses below their yield limits. In other words, compliant and strong designs are deemed more appropriate than optimally flexible and stiff designs.

In this article, to obtain compliant and strong (failure-free) designs, local failure issues of monolithic compliant mechanisms are addressed by employing stress constraints in their topology design. Section II describes the problem statement of compliant mechanisms with stress constraints. Section III is a brief review of relevant work on topology optimization of stiff structures with stress constraints followed by its extension to a compliant topology design. Numerical difficulties with the implementation of stress constraints are noted and avoided using the quality functions and stress constraint relaxation. In the subsequent sections, three synthesis examples for compliant mechanisms are discussed and compared with solutions obtained using existing multicriteria formulations. Finally, a fully stressed design approach based on an optimality criteria is incorporated to render the resultant topologies manufacturable.

II. PROBLEM STATEMENT

Consider an arbitrary design domain with generic loading and boundary conditions shown in Fig. 2. P_2 is the point of output deformation along the prescribed direction. A spring of constant k_s models the work piece at the output port. For linear finite-element models, the output deformation or the mutual strain energy MSE can be computed using the unit dummy load method [15] as

$$MSE = \mathbf{V}^T\mathbf{K}\mathbf{U} \tag{3}$$

with

levels below their upper bound unless a stress constraint is applied. There is, however, another way of using compliant structures such as in leaves and thin tree branches, marine algae [12], and deepwater offshore structures that are used in oil and natural gas industry [13] these are able to reduce local stresses when subjected to large water or wind currents. These compliant structures prefer to comply with the external loads, allowing large rigid-body displacements but minimal local distortions, thus maintaining the stresses below the yield limit.

The aforementioned stress reduction phenomenon can be explained for both stiff and compliant structures using the cantilever beam example shown in Fig. 1. For a beam loaded with a point tip force P, elastic modulus E, in-plane width b, and out-of-plane thickness t, the maximum stress σ_{max} occurs at the fixed end, which is given as

$$\sigma_{max} = 6aP/tb^2 \tag{1}$$

where a is the horizontal distance from the fixed end to the deflected tip and is given using the large deformation Euler-Lagrange beam theory as [1]

$$\sqrt{\frac{Etb^3}{24P}}\int_0^{\theta_o}\frac{\cos\theta}{\sqrt{\sin\theta - \sin\theta}} \tag{2}$$

with θ_o as the slope at the tip (see [14] for derivation details). For given tip load P, σ_{max} can be reduced by lowering $a/(tb^2)$. By using Eq. 2, this can be accom-

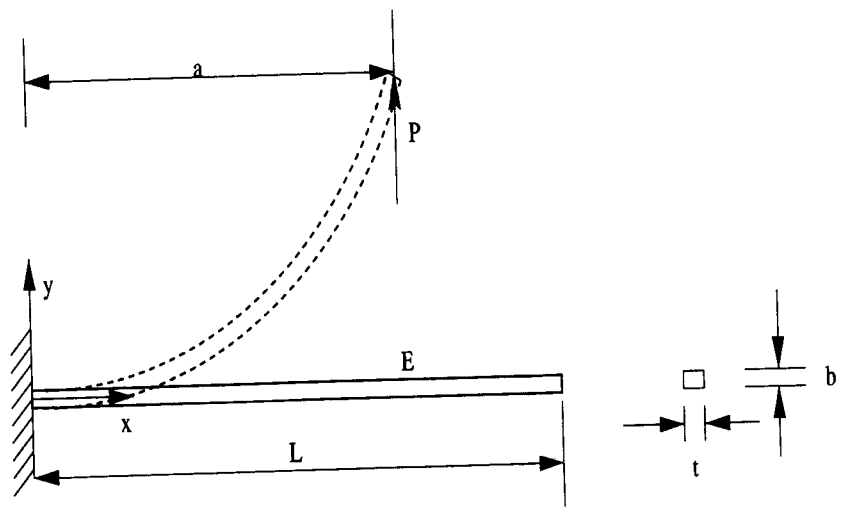

Figure 1. A simple cantilever beam example demonstrating modes of stress reduction in stiff and compliant structures.

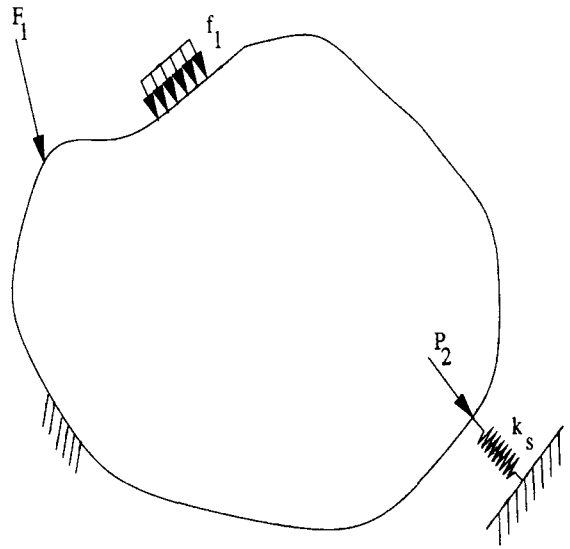

Figure 2. Design domain and problem specifications.

$$\mathbf{KU} = \mathbf{F}_a$$
$$\mathbf{KV} = \mathbf{F}_d \tag{4}$$

where $\mathbf{U}$ is the displacement field due to the load vector $\mathbf{F}_a$ comprising applied loads, $\mathbf{K}$ is the structural stiffness matrix, and $\mathbf{V}$ is the displacement field due to the load vector $\mathbf{F}_d$, which is the unit dummy load that acts along the direction of the prescribed output deformation. The stress σ_i in element i can be written as

$$\sigma_i = \mathbf{D}_i\mathbf{B}_i\mathbf{u}_i \tag{5}$$

Here, $\mathbf{D}_i$ is the elastic constitutive matrix, $\mathbf{B}_i$ is the strain displacement matrix, and $\mathbf{u}_i$ is the nodal deformation of the ith element. For topology design of compliant mechanisms, the flexibility requirement can be posed as maximizing the output deformation, while strength requirements can be imposed using an upper bound on stresses for elements that are retained in the optimal topology. That is,

Maximize: *MSE*

subject to

$$|\sigma_i| \le \sigma_a = \frac{S_y}{SF}, \qquad \text{for } x_i > x_l$$

$$V \le V^*$$
$$x_l \le x_i \le x_u, \qquad i = 1, \ldots, N$$

where σ_a is the allowable stress, S_y is the yield strength with a safety factor SF, N is the total number of elements in domain representation, V^* is an upper bound on the continuum volume V, and x_l and x_u are lower and upper bounds on design variables x_i ($i = 1, \ldots, N$), respectively. These variables can be related to element thicknesses or widths or their Young's moduli. Design variables assuming the lower bound are considered absent from the topology. Even though the lower bound should ideally be zero, it is taken as a small positive quantity to avoid singularities in structural stiffness.

III. MODELING STRENGTH CONSTRAINTS

Stress constraints have been employed in recent work on topology optimization of stiff structures [16–19] and size optimization of compliant mechanisms [20]. Kirsch [16] and Cheng and Jiang [17] performed topology optimization using a ground structure of truss elements and found that, for a bar element, the axial stress asymptotically approaches a nonzero finite value as the element approaches its nonexisting state. As explained by Cheng and Jiang [17], the nodes of a nonexisting element may be shared by those existing in the mesh.

Consider, for instance, a nonexisting element shown using dotted lines in a mesh of truss elements (solid lines) in Fig. 3. Unless otherwise constrained by zero displacement boundary conditions, nodes a and b will undergo finite deformations due to the applied load P. The stress σ_e in the nonexisting element e will be a nonzero finite value given as

$$\sigma_e = E_e \frac{u_b^{\text{axial}} - u_a^{\text{axial}}}{L_e} \tag{6}$$

where L_e is the element length, E_e is its elastic modulus, and u_a^{axial} and u_b^{axial} are the deformations of nodes a and b, respectively, along the length of the element. Duysinx and Bendsøe [18] noted similar asymptotic behavior of local microscopic stresses for rank 2 microstructures and plane stress design parameterization. Kirsch [16] referred to this phenomenon as a *singularity* because the element stresses assume nonzero values at their nonexisting states, which are situations in which stress values are expected to vanish. Such degeneracies create complex design regions comprising several unconnected parts. The design contains disconnected segments for which the constraint qualification for the existence of a feasible minimum is not satisfied [18]. In such cases, the optimization algorithms based on Karush-Kuhn-Tucker conditions are unable to reach

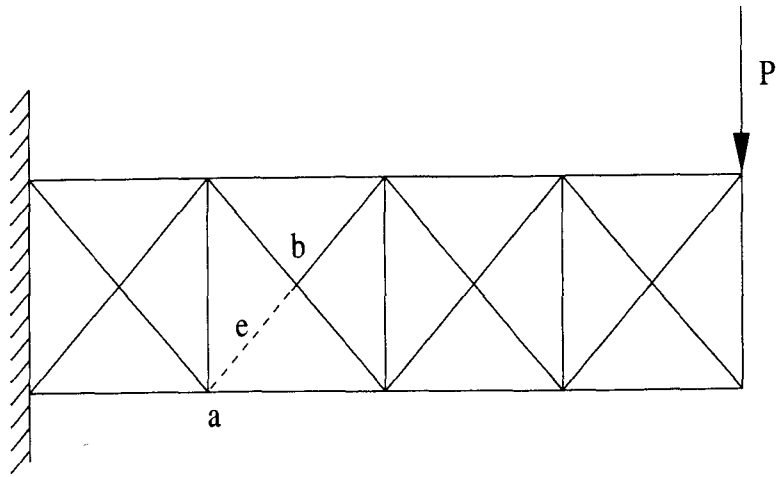

Figure 3. Asymptotic behavior of stresses in a bar element in its nonexisting state.

the optima located in these regions. This implies that, in topology optimization, some low-density regions are not removedtotally.

To overcome these irregularities, Kirsch [16] suggested employing upper limits on internal forces instead of element stresses. For a truss element, the internal force is a product of the stress and its area of cross section. When the cross-sectional area approaches zero or the element approaches its nonexisting state, the internal force approaches zero. Cheng and Jiang [17] generalized this approach by proposing to use the quality functions in conjunction with the stress constraints. Like the cross-sectional area of the truss element, the quality functions for individual elements are chosen as continuous, monotonic, and positive functions in the respective design variables and have a null (zero) value for variables attaining their lower limits. These quality functions may be regarded as respective weights or switch functions for stress constraints. For elements that are retained in the topology, these weights are large, implying that the failure criteria are strict for elements that are significant in the topology. For elements that are near their nonexisting state, the failure criteria are relaxed by reducing the weights to help in smooth disappearance of such elements from the topology.

The models described above can be adapted for the topology synthesis of compliant mechanisms. First, element densities ρ_i $(i = 1, \ldots, N)$ can be expressed in terms of design variables x_i $(i = 1, \ldots, N)$ as

$$\rho_i = \frac{x_i - x_l}{x_u - x_l}, \qquad i = 1, \ldots, N \tag{7}$$

where $\rho_i = 0$ signifies a nonexisting ith element and existing otherwise ($\rho_i > 0$). Quality functions q_i can be chosen to depend monotonically on element densities such that

$$q_i = f(\rho_i)\begin{cases} = 0 & \text{for } \rho_i = 0 \\ > 0 & \text{for } \rho_i > 0 \end{cases} \tag{8}$$

Some candidate choices for q_i are exponential or polynomial functions [17], that is, $q_i = (e^{\rho_i} - 1)$ or $q_i = \rho_i^n$. Polynomial functions are chosen in this work because they offer additional flexibility in choosing weights for stress constraints in selecting parameter n. On multiplying both sides of the stress constraints with respective quality functions and rearranging, we get

$$\rho_i^n\left(\frac{|\sigma_i|}{\sigma_a} - 1\right) \le 0, \qquad i = 1, \ldots, N \tag{9}$$

Stress relaxation, proposed by Cheng and Guo [21] and used by Duysinx and Bendsøe [18], can be employed to circumvent the degeneracies due to the asymptotic nature of stress constraints to aid in easy removal of elements approaching their nonexisting state. Expressing Eq. 9 in the relaxed form for a small relaxation parameter ε, we have

$$\rho_i^n\left(\frac{|\sigma_i|}{\sigma_a} - 1\right) \le \varepsilon, \qquad i = 1, \ldots, N \tag{10}$$

By analyzing its arranged form, that is,

$$|\sigma_i| \le \sigma_{a(\text{relaxed})} = \sigma_a\left(1 + \frac{\varepsilon}{\rho_i^n}\right), \qquad i = 1, \ldots, N \tag{11}$$

it can be observed that, for nonzero densities and positive ε, stress values are not allowed to exceed their redefined allowable limit, $\sigma_{a(\text{relaxed})} = \sigma_a(1 + \varepsilon/\rho_i^n)$, which is only slightly larger than the allowable stress σ_a if ε is small and n is chosen properly (Fig. 4). However, for densities ρ_i approaching zero, the upper bounds on local stresses approach infinity. In other words, the stress constraints on elements approaching their nonexisting state are inactive. ε-Relaxation thus permits element densities to approach their lower bound smoothly by relaxing the respective stress constraints, thus yielding a regular design space with well-placed optima that can be found with classical mathematical programming algorithms. Cheng and Guo [21] mentioned that the constraint relaxation creates

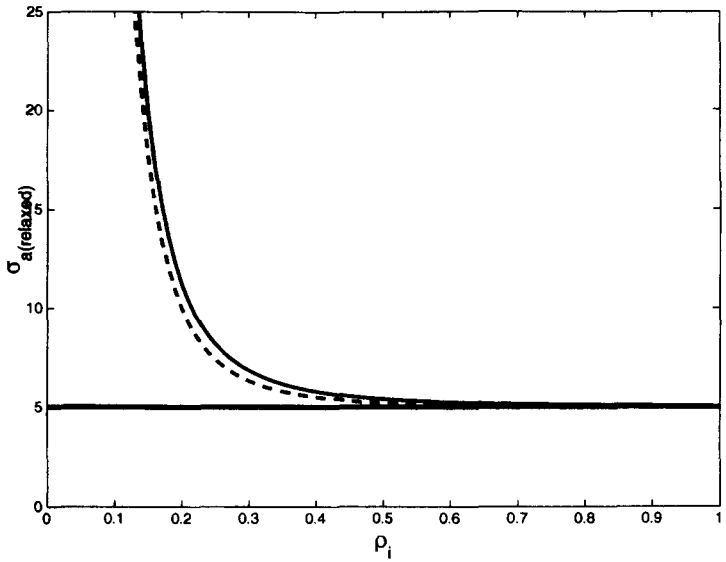

Figure 5. *Solid curve*: Relaxed upper bound on stress, $\sigma_a(1 + \varepsilon/\rho_i^n)$ plotted against ρ_i. *Dashed curve*: Relaxed upper bound $\sigma_a(1 + \varepsilon(1 - \rho_i)/\rho_i^n)$. $\varepsilon = 0.01$ and $\sigma_a = 5$.

$$\rho_i^n\left(\frac{|\sigma_i|}{\sigma_a} - 1\right) \le \varepsilon(1 - \rho_i)$$

$$V \le V^*$$

$$x_l \le x_i \le x_u, \qquad i = 1, \ldots, N$$

Duysinx and Bendsøe [18] related the relaxation parameter ε to the lower bound on design variables as $x_l = \varepsilon^2$ and progressively decreased ε. They mentioned that choosing a large initial ε, and thus the lower bound, allows one to open degenerate parts to find a single optimum from most initial guesses. A way to decrease ε proposed by Duysinx and Sigmund [22] is to do so each time the Lagrangian of the objective and constraints satisfies the convergence criteria. This requires solving the optimization problem iteratively with the solution of the previous step as the initial for subsequent guess optimization. Both Duysinx and Bendsøe [18] and Duysinx and Sigmund [22] used $n = 3$ for density-based plane stress parameterization in concurrence with the penalization parameter for the element densities.

However, parameter n can be chosen on the basis of the relaxed bound on the stress $\sigma_{a(\text{relaxed})}$ ($> \sigma_a$) desired at a given density value ρ_o bounded by the interval [0, 1] (see Fig. 4). Following from Eq. 11, for the lowest value of the

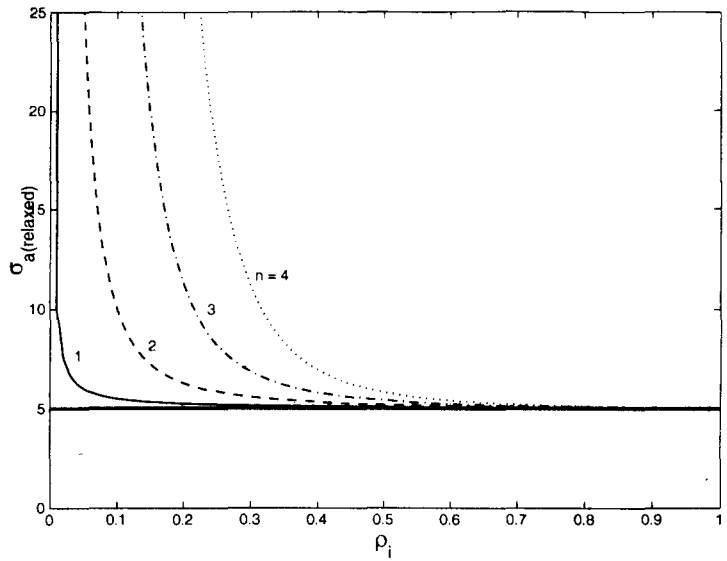

Figure 4. Relaxed upper bounds on stresses, $\sigma_a(1 + \varepsilon/\rho_i^n)$ plotted against ρ_i for different values of n. In the schematic, $\varepsilon = 0.01$ and $\sigma_a = 5$.

continuous point-to-set maps between parameter ε and the relaxed design domains, as well as their optimal solution that regularizes the design space.

Duysinx and Sigmund [22] noted that relaxation of the strength constraints may not be required for element densities ρ_i ($i = 1, \ldots, N$) closer to unity and proposed that stresses for such elements be strictly bounded by the allowable stress σ_a. Accordingly, Eq. 10 can be modified as follows:

$$\rho_i^n\left(\frac{|\sigma_i|}{\sigma_a} - 1\right) \le \varepsilon(1 - \rho_i), \qquad i = 1, \ldots, N \tag{12}$$

Figure 5 shows the comparison between the relaxed upper bounds on the stress with element density. In the figure, the solid curve corresponds to the model in Eq. 10 with constant relaxation parameter, and the dotted line represents the relaxed upper bound for the relaxation parameter varying linearly with the element density as in Eq. 12. With relaxation incorporated with stress constraints, the optimization problem for compliant mechanisms can be posed as follows:

Maximize: *MSE*

subject to:

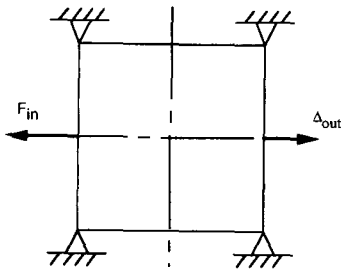

(a)

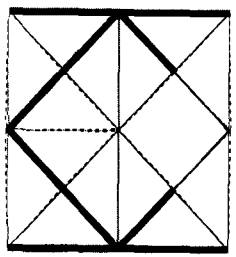

(b) maximum stress = 37.83 N/mm^2

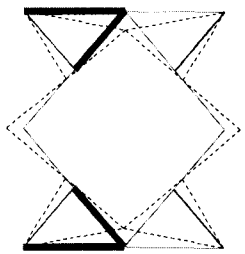

(c) maximum stress = 42.08 N/mm^2

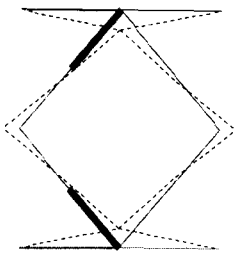

(d) maximum stress = 39.57 N/mm^2

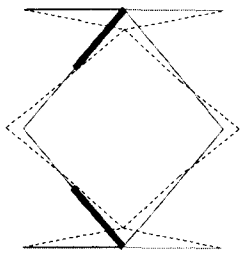

(e) maximum stress = 40.27 N/mm^2

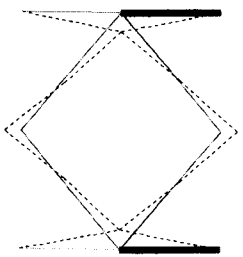

(f) maximum stress = 38.3 N/mm^2

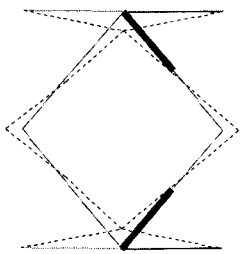

(g) maximum stress = 35.2 N/mm^2

Figure 6. (a) Design specifications for the displacement inverter. (b)–(g) Optimal topologies for n varying from 1 to 6.

relaxation parameter ε (if it is reduced periodically as described above), n can be computed as follows:

$$n = \frac{log(\varepsilon) - log\left(\frac{\sigma_{a(\text{relaxed})}}{\sigma_a} - 1\right)}{log(\rho_o)} \tag{13}$$

Note that, in maximizing the flexibility (or the output deformation) in the topology design of compliant mechanisms, many element densities are expected to be close to their lower bound, but the corresponding elements may still be significant and thus retained in the optimal topology. The stresses in such elements may be larger than their allowable limit σ_a owing to the artificial relaxation of their upper bounds achieved by using the quality functions and the relaxation parameter ε. To avoid the stress levels in these elements from exceeding their yield limit S_y, σ_a can be artificially chosen to be much smaller than S_y (by a factor of 5 or more). This conservative approach will ensure that most of the existing elements have stresses below S_y. With appropriate resizing following the topology optimization procedure, the stress levels can be further regulated with the yield limit as the upper bound on stresses, will be explained below.

In this article, synthesis examples for displacement inverter, compliant crimper, and pliers mechanisms are studied. Frame elements were chosen for design parameterization for their simplicity yet nontriviality in continuum representation and implementation. In-plane widths are regarded as design variables for elements. Stresses in frame elements also depict irregularities mentioned above in that they approach the nonzero axial stress value at zero densities and behave similarly to bar elements. Thus, the model to handle stress constraints developed in this section is applicable to frame elements as well. Young's modulus for elements was chosen as 2×10^3 N/mm^2, yield stress S_y for elements was 50 N/mm^2, and the allowable stress σ_a was taken as 10 N/mm^2. An upper bound of 4 mm was imposed on design variables of frame elements of constant thickness 2 mm. A uniform initial guess equal to half the upper bound on the design variables was employed in the synthesis examples. The examples were obtained using sequential quadratic programming in Matlab [23] and were studied for constant and progressively varying stress relaxation parameter and different values of parameter n.

IV. SYNTHESIS EXAMPLES

A. Displacement Inverter

Figure 6a shows the design domain of dimensions 120 mm × 120 mm for a displacement inverter. The rectangular region is pinned at four corners and

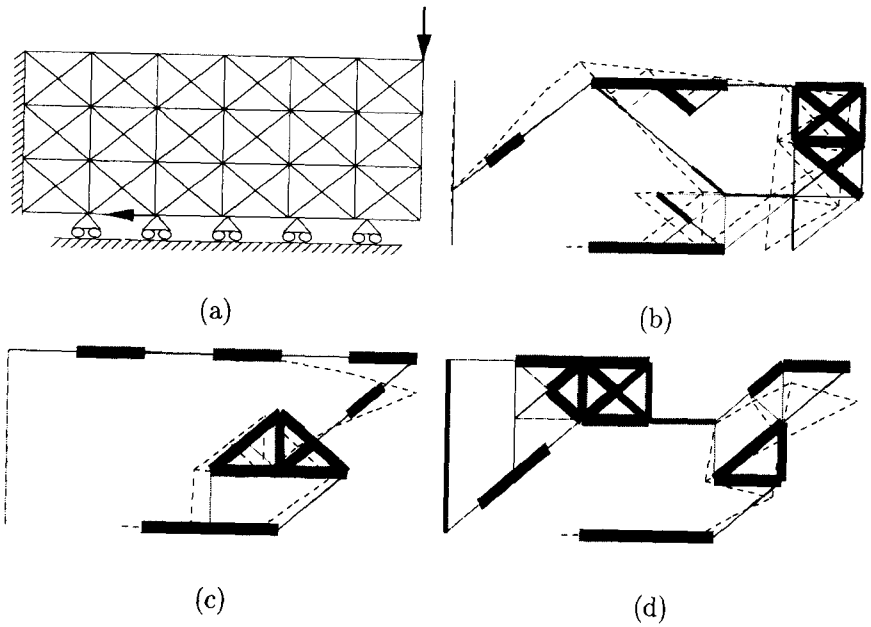

Figure 7. (a) Design specifications for the compliant crimper. (b) Optimal topology for $n = 1$ and volume constraint of 30%. (c) Optimal topology for $n = 3$ and volume constraint of 30%. (d) Optimal topology for $n = 3$ and no volume constraint.

The optimal topology for $n = 1$ is shown in Fig. 7b, for which the output deformation was maximized to 14.5 mm. A volume constraint of 30% was imposed for this design.

Figures 7c and 7d show optimal topologies for $n = 3$, with 30% volume constraint applied in the former and no resource constraint applied in the latter. The output displacements for topologies in Figs. 7c and 7d were maximized to 45.2 mm and 41.9 mm, respectively. Large values of optimal output displacements are due to thin elements in the topologies allowed by the relaxed failure criteria.

For the three optimal solutions, the relaxation parameter ε was held fixed at 0.01, and the lower bound on the design variables was taken to be 10^{-3} mm. The three topologies are quite well defined, although in the topology in Fig. 7b some elements, especially in the lower right corner, were retained that restrict the flexibility of the continuum by not allowing sufficient input deformation, consequently making it stiffer. For $n = 3$ (Figs. 7c and 7d), resultant topologies were more flexible. Again, for large n, stress levels in some thin elements ex-

discretized using a ground structure of frame elements as shown. The input load F_{in} of 20 N was applied at the center node on the left edge, and the deformation of the center node on the right edge was desired to be maximized. A spring constant of 0.01 N/mm was used at the output port. No volume constraint was imposed in this example. The relaxation parameter ε was gradually reduced from 10^{-1} to 10^{-4} by a factor of 5, and in each optimization step, the lower bound $x_l = \varepsilon^2$ was imposed on in-plane element widths.

Figures 6b–6g show optimal topologies of displacement inverter for n varying from 1 to 6. The solid lines in these figures show the undeformed configuration with relative element in-plane widths, while the normalized deformed configuration is shown using dotted lines. For $n = 1$, the optimal topology is shown in Fig. 6b, for which the output displacement is maximized to 0.88 mm. As n increases from 2 to 6, the corresponding output displacements are maximized to 106.8 mm, 114.7 mm, 114.7 mm, 114.8 mm, and 114.8 mm, respectively.

The optimal topologies are shown in Figs. 6c–6g. As is apparent in these figures, with increasing n, the optimal topologies became more flexible and better defined. This is because the unfavorable element densities were pushed to their lower bounds more quickly owing to the polynomial nature of the quality functions. The high values of output displacements in Figs. 6c–6g can be attributed to the presence of very thin elements in the corresponding topologies.

Note that, for such elements, the failure criteria were not very strict. This is expected because of the relaxation of the upper bounds on local stresses, discussed in Section III. Consequently, local stresses were larger than the allowable limit of 10 N/mm^2. Since σ_a was chosen to be much smaller than the yield strength in anticipation of the stress relaxation for thin elements, the local stresses were still bounded by the yield strength. The example also shows that increasing n did result in more flexible and clear topologies. However, after a certain value ($n \geq 3$ in this example), convergence in the optimal topologies could be seen.

B. A Compliant Crimper

The symmetric half of the design region for the crimper is depicted in Fig. 7a. The region is rectangular, 150 mm long and 50 mm wide. The left edge of the domain was fixed, while the bottom edge was on a roller support due to symmetry. A vertically downward input force of 20 N was applied at the top right corner, which is indicated by a dark arrow. The gray arrow pointing toward the left at the bottom edge depicts the location and direction of the output displacement to be maximized. An output spring of constant 0.01 N/mm was used to model the reaction load from the work piece.

ceeded their allowable limit of 10 N/mm^2, but were lower than the prescribed limit of 50 N/mm^2.

The crimper example was also solved with $n = 3$ and no volume constraint for varying ε. Here, the relaxation parameter was progressively decreased in multiple optimization steps from 10^{-1} to 10^{-4}. The optimal solution is shown in Fig. 8, in which the output deformation was maximized to 44.8 mm. Stress levels were contained within the yield limit. The resultant solution is better than the solution shown in Fig. 7d, suggesting that a progressive decrease in the relaxation parameter generates better topologies, notwithstanding the higher computational costs.

C. Compliant Pliers

A rectangular region of 150 mm by 50 mm, which is the symmetric half of the design domain, was used for synthesis of compliant pliers. The region was discretized as shown in Fig. 9a, with its bottom edge fixed. Input forces of 2 N and −20 N, indicated by dark arrows, were applied for actuation along the horizontal and vertical directions at the top left corner of the domain. The output deformation at the bottom right node was desired to be maximized along the direction at −45° from the horizontal. This is shown by two gray arrows at the output port. Output springs of 0.01 N/mm and 0.1 N/mm were employed along the vertical and horizontal directions, respectively. Owing to uneven spring constants, the output port was expected to deform more along the vertically downward direction than toward the right. Figure 9b shows the optimal topology for $n = 1$, for which the solution was slightly ambiguous, although the objective was maximized to 15.4 mm. Much clearer topologies were obtained for $n = 3$ in Fig. 9c with 30% volume constraint and in Figs. 9d and 9e for $n = 3$ and $n = 4$, respectively, with no volume constraint. The output deformations were maximized to 85.1 mm, 68.3 mm, and 62.5 mm, respectively.

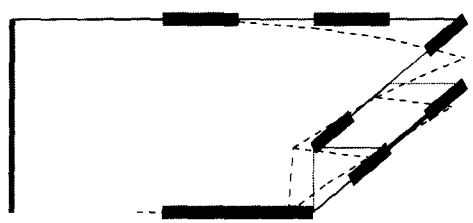

Figure 8. Optimal topology for compliant crimper for $n = 3$ with no volume constraint. ε is progressively reduced from 0.1 to 10^{-4}.

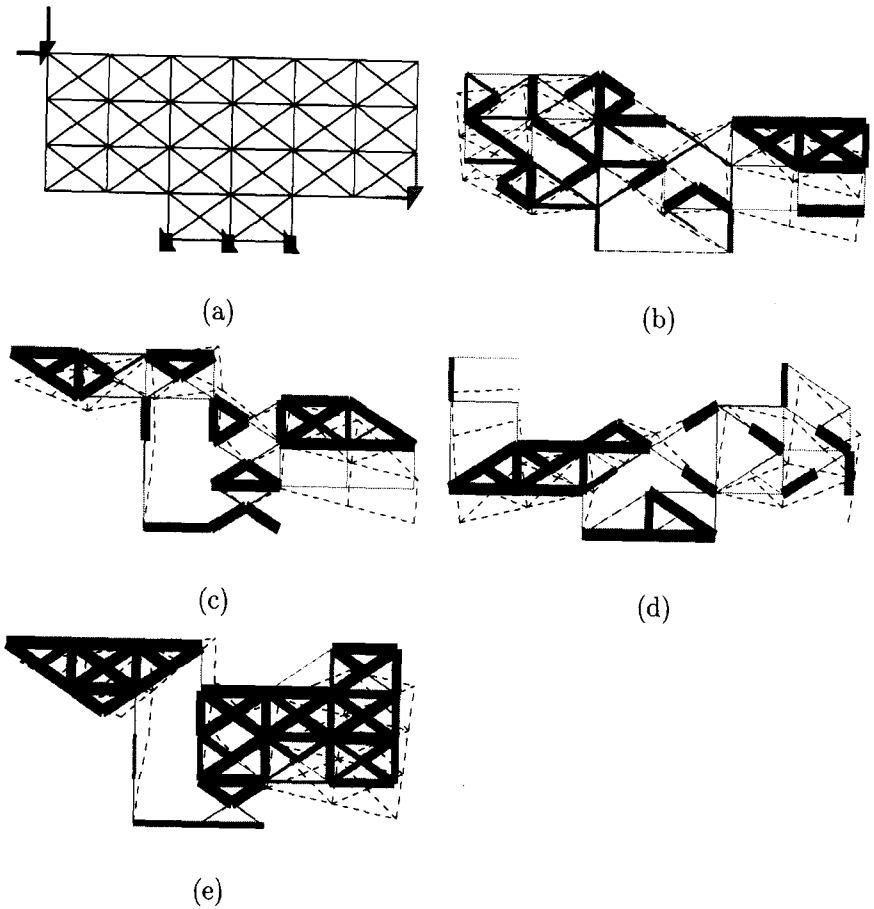

Figure 9. (a) Design specifications for the compliant pliers. (b) Optimal topology for $n = 1$ and volume constraint of 30%. (c) Optimal topology for $n = 3$ and volume constraint of 30%. (d) Optimal topology for $n = 3$ and no volume constraint. (e) Topology for $n = 4$ and no volume constraint.

The aforementioned pliers designs were obtained for fixed $\varepsilon = 0.01$ and $x_l = 10^{-3}$ mm. The problem was solved with the relaxation parameter varying from 0.1 to 10^{-4} and the lower limit varying as ε^2 in each optimization step. In this case, $n = 3$ was used without the volume constraint. Optimal topology is shown in Fig. 10, in which the output deformation was maximized to 530 mm and compared better with the solution depicted in Fig. 9d.

proach [6], for which the deformation at the output port was 40.6 mm, and element stresses were less than the yield strength. When compared with Fig. 8, this optimal mechanism was equally flexible and failure free for prescribed loading conditions. This example suggests that the individual dominance of flexibility and stiffness objectives depends on the choice of the measuring functions.

Though minimizing the strain energy does help in restricting the stress levels, flexibility-stiffness solutions do not always guarantee designs against failure, as is demonstrated in the subsequent example. For compliant pliers, the resultant topology obtained using the energy formulation is shown in Fig. 12. At optimum, output deformation was 82 mm, and the strain energy was 475.6 N-mm. Maximum stress levels exceed the yield strength by fivefold, whereas the resultant mechanism was less flexible when compared with the solution in Fig. 10.

VI. DISCUSSION

Many times, thin and nonmanufacturable elements may be present in the optimal topology obtained using stress constraints. Local stresses in thin elements may exceed the yield strength, depending on the choice of parameter n, the stress relaxation parameter ε, and the allowable stress limit σ_a. Furthermore, the quality functions and relaxation parameter only help to ignore the local stresses in nonexisting, but physically present, elements in the mesh. Such elements may be highly stressed and may share the applied loads to some extent. When removed, these stresses may be transferred to existing elements, making their stress levels higher.

To further restrain these stresses within their yield limit and ensure that the minimum element size conforms with the manufacturing limit, an optimality criteria method such as fully stressed design [24] may be incorporated. Assuming that local stresses are inversely proportional to their design variables, the element size may be increased iteratively by a factor equal to the ratio of the

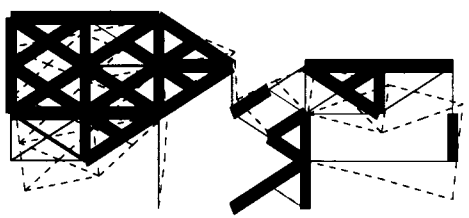

Figure 12. Optimal topology for compliant pliers with the energy formulation.

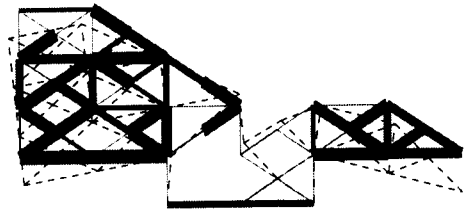

Figure 10. Optimal topology for compliant pliers for $n = 3$ with no volume constraint. ε is progressively reduced from 0.1 to 10^{-4}.

V. OPTIMAL TOPOLOGY COMPARISON WITH FLEXIBILITY-STIFFNESS FORMULATIONS

Optimal topologies were obtained for compliant crimper and pliers mechanisms for specifications in Figs. 7a and 9a using the flexibility-stiffness formulation proposed by Frecker et al. [4] and Saxena and Ananthasuresh [6]. The topologies were obtained without the volume constraint. Figure 11a shows the topology of an optimal crimper mechanism obtained by maximizing the ratio of the output deformation and strain energy. The mutual energy was maximized to 4.2 mm, whereas the strain energy was minimized to 9.2 N-mm. The maximum stress was found to be less than the yield strength (50 N/mm^2).

Even though the mechanism was not designed against failure in this example, the stresses were restricted by indirectly constraining the input deformation by minimizing the mean compliance. However, on comparing the flexibility of the optimal crimpers in Figs. 8 and 11a, it is found that the output deformation of the mechanism obtained by using stress constraints is about 10 times more for the design in Fig. 8 than the design in Fig. 11a.

A crimper mechanism was also generated using the energy-based ap-

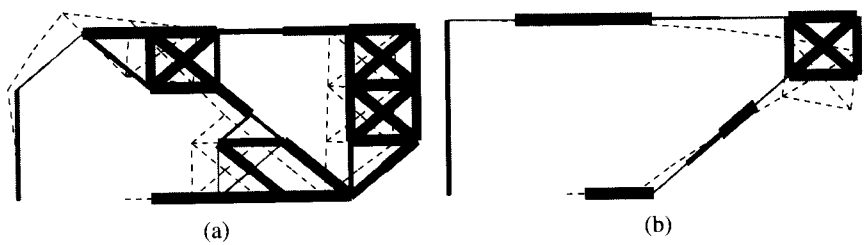

Figure 11. Optimal topology for compliant crimpers. (a) Ratio formulation. (b) Energy formulation.

local stress to the yield stress if the former is greater. Appropriate checks may then be performed in each iteration to ensure that the element sizes lie within the limits defined by the manufacturing constraint and their upper bound.

Fully stressed designs were obtained for topologies of compliant crimper and pliers in Figs. 8 and 10, respectively. The yield stress of 50 N/mm^2 was used with a minimum element in-plane width (manufacturing limit) of 2 mm. The upper bound of 5 mm was used on the element sizes. Figs. 13a and 13b show the fully stressed designs of compliant crimper and pliers, respectively. For the crimper example, the maximum stress was reduced from 1711 N/mm^2 to 58.4 N/mm^2. An initially high value of the maximum stress may be because the nonexisting elements may be highly stressed and sharing a large part of applied loads. The resultant value was still larger than the yield strength and can be attributed to the lower values of the element thickness and/or the upper bound used on the element in-plane widths. Ideally, the upper bound on design vari-

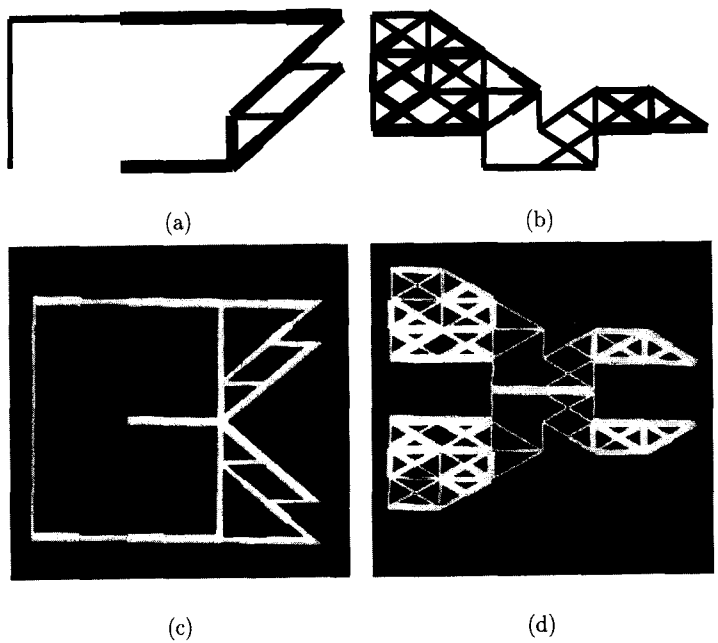

Figure 13. Fully stressed designs of compliant (a) crimper and (b) pliers and their prototypes (c) and (d), respectively.

ables is not necessary for the fully stressed design procedure as it aims to minimize the continuum volume while rendering the constituting members in the topology fully stressed.

Further reduction in stresses below the yield strength is possible by either having no upper bound on element widths or using out-of-plane thicknesses larger than 2 mm. For a thickness of 4 mm, the maximum stress was reduced to 27.7 N/mm^2. In the case of pliers, stress reduction was from 690 N/mm^2 to 14 N/mm^2, which is less than the yield strength. The output deformation after resizing was 4.6 mm. Resizing was also performed on the topology of Fig. 12, obtained using the energy formulation in which the maximum stress was reduced from 229 N/mm^2 to 26.1 N/mm^2, yielding the output deformation to 3.1 mm. This is smaller than the 4.6 mm obtained as output deformation for the resized topology in Fig. 13b. Note that all the examples in this article were solved using linear finite-element models in which the stress estimate is more conservative than when the corresponding geometrically nonlinear finite elements are used.

VII. CONCLUSIONS

Flexibility-stiffness formulations do not directly address the local failure issues in the topology design of compliant mechanisms. Furthermore, if flexibility and stiffness measures are not properly chosen, optimal compliant topologies can be overly stiff. It then becomes imperative to employ an upper bound (the allowable limit) on local stresses for existing elements in the topology. Local stresses for different design parameterization, including truss, frame, and plane stress elements, manifest some irregularities in that they asymptotically approach a nonzero finite value when the corresponding element densities approach a null value.

Quality functions are employed to help impose stress constraints only for nonzero element densities in the optimization procedure. Stress constraints are also relaxed by a known parameter to regularize the design space, thus helping the mathematical programming algorithms approach more meaningful topologies.

Numerous topology design examples for compliant mechanisms were solved in this paper with stress constraints and were compared with corresponding solutions obtained using the flexibility-stiffness multicriteria formulations. Topologies obtained using strength considerations were found to be more flexible, with local stress levels contained within the specified yield limit compared to those obtained using prior flexibility-stiffness formulations.

REFERENCES

1. Howell, L.L.; Midha, A. Parametric Deflection Approximations for End Loaded, Large Deflection Beams in Compliant Mechanisms. ASME J. Mech. Design **1995**, *117*, 156–165.
2. Ananthasuresh, G.K.; Kota, S. Designing Compliant Mechanisms. Mech. Eng. **1995**, *117* (11), 93–96.
3. Ananthasuresh, G.K. A New Design Paradigm for Micro-Electro-Mechanical Systems and Investigations on Compliant Mechanisms Synthesis; Ph.D. thesis; University of Michigan: Ann Arbor, MI, 1994.
4. Frecker, M.I.; Ananthasuresh, G.K.; Nishiwaki, N.; Kikuchi, N.; Kota, S. Topological Synthesis of Compliant Mechanisms Using Multi-Criteria Optimization. ASME J. Mech. Design **1997**, *119* (2), 238–245.
5. Sigmund, O. On the Design of Compliant Mechanisms Using Topology Optimization. Mech. Struct. Mach. **1997**, *25* (4), 495–526.
6. Saxena, A.; Ananthasuresh, G.K. On an Optimal Property of Compliant Mechanisms. Struct. Multidisciplinary Optimization **2000**, *19* (1), 36–49.
7. Barnett, R.L. Minimum Weight Design of Beams for Deflection. J. Eng. Mech. Div., Proc. Am. Soc. Civil Eng. **1961**, *EM1*, 75–109.
8. Frecker, M.I.; Kota, S.; Kikuchi, N. Use of Penalty Function in Topological Synthesis and Optimization of Strain Energy Density of Compliant Mechanisms. *Proceedings of the ASME Design Engineering Technical Conferences, Sept. 14–17, Sacramento, California, DETC97/DAC 3760*, 1997.
9. Saxena, A.; Ananthasuresh, G.K. An Optimality Criteria Approach for the Topology Synthesis of Compliant Mechanisms. *Proceedings of the DETC'98, ASME Design, Engineering Technical Conference, Sept. 13–16, Atlanta, Georgia, DETC98/MECH-5937*, 1998.
10. Canfield, S.; Frecker, M. Design of Compliant Mechanisms for Amplification of Induced Strain Actuators. *Proceedings of the 1999 ASME Design Engineering Technical Conferences Sept. 12–15, 1999, Las Vegas, Nevada, Paper DETC99/DAC-860*, 1999.
11. Sandor, B.I. *Strength of Materials*; Prentice Hall: Englewood Cliffs, NJ, 1978.
12. Vogel, S. Better Bent Than Broken. Discover **1995**, *May*, 62–67.
13. Bar-Avi, P.; Benaroya, H. *Nonlinear Dynamics of Compliant Offshore Structures*, Swets & Zeitlinger: Lisse, Netherlands, 1997.
14. Saxena, A.; Kramer, S.N. A Simple and Accurate Method for Determining Large Deflections in Compliant Mechanisms Subjected to End Forces and Moments. ASME J. Mech. Design **1998**, *120* (3), 392–400.
15. Shield, R.T.; Prager, W. Optimal Structural Design for Given Deflection. J. Appl. Math. Phys., *ZAMP* **1970**, *21*, 513–523.

16. Kirsch, U. On Singular Topologies in Optimum Structural Design. Struct. Optimization **1990**, *2*, 133–142.
17. Cheng, G.D.; Jiang, Z. Study on Topology Optimization with Stress Constraints. Eng. Optimization **1992**, *20*, 129–148.
18. Duysinx, P.; Bendsøe, M.P. Topology Optimization of Continuum Structures with Local Stress Constraints. Int. J. Numer. Methods Eng. **1998**, *43* 1453–1478.
19. Yunkang, S.; Xin, Y. The Topological Optimization for Truss Structures with Stress Constraints Based on the Exist-Null Combination. Acta Mech. Sinica **1998**, *14* (4), 363–370.
20. Hetrick, J.A.; Kota, S. An Energy Formulation for Parametric Size and Shape Optimization of Compliant Mechanisms. ASME J. Mech. Design **1999**, *121* (2), 229–234.
21. Cheng, G.D.; Guo, X. ε-Relaxation Approach in Structural Optimization. Struct. Optimization **1997**, *13*, 258–266.
22. Duysinx, P.; Sigmund, O. New Developments in Handling Stress Constraints in Optimal Material Distributions. *Seventh Symposium in Multidisciplinary Analysis and Optimization, AIAA/USAF/NASA/ISSMO, AIAA-98-4906, Sept.* 1998; 1501–1509.
23. *The Language of Technical Computing*, Student Ed., 5th Ed., The MathWorks, Inc.: Natick, MA, 2000.
24. Haftka, R.J.; Gürdal, Z. *Elements of Structural Optimization*; Kluwer Academic Publishers: Boston, 1989.

Received April 2000
Revised September 2000